frontiers | Frontiers in Earth Science

ORIGINAL RESEARCH
published: 28 April 2022
doi: 10.3389/feart.2022.901989

Implication of Alkane Carbon and Hydrogen Isotopes for Genesis and Accumulation of Over-Mature Shale Gas: A Case Study of Longmaxi Formation Shale Gas in Upper Yangtze Area

Zhipeng Chen[1,2], Yun Liao[1], Li Liu[3], Lei Chen[4,5], Pengtao Wang[6], Yinhui Zuo[2], Zhanli Ren[7], Lianqi Jia[7] and Wei Dang[1]*

[1]School of Earth Sciences and Engineering, Xi'an Shiyou University, Xi'an, China, [2]State Key Laboratory of Oil and Gas Reservoir Geology and Exploitation, Chengdu University of Technology, Chengdu, China, [3]Research Institute of Petroleum Exploration and Development, Petrochina, Beijing, China, [4]Shandong Provincial Key Laboratory of Deep Oil and Gas, Qingdao, China, [5]School of Geosciences, China University of Petroleum (East China), Qingdao, China, [6]Sinopec Green Source Thermal Energy Development Co., Ltd., Xianyang, China, [7]Department of Geology, Northwest University, Xi'an, China

OPEN ACCESS

Edited by:
Dongdong Liu,
China University of Petroleum, Beijing, China

Reviewed by:
Zhaodong Xi,
China University of Geosciences, China
Rui Yang,
China University of Geosciences Wuhan, China

***Correspondence:**
Lei Chen
chenlei19880804@163.com

Specialty section:
This article was submitted to Economic Geology, a section of the journal Frontiers in Earth Science

Received: 22 March 2022
Accepted: 13 April 2022
Published: 28 April 2022

Citation:
Chen Z, Liao Y, Liu L, Chen L, Wang P, Zuo Y, Ren Z, Jia L and Dang W (2022) Implication of Alkane Carbon and Hydrogen Isotopes for Genesis and Accumulation of Over-Mature Shale Gas: A Case Study of Longmaxi Formation Shale Gas in Upper Yangtze Area. Front. Earth Sci. 10:901989. doi: 10.3389/feart.2022.901989

To clarify the implication of alkane carbon and hydrogen isotopes for the genesis and accumulation of over-mature shale gas, we carried out a comparative study on Longmaxi shale gases from eight blocks in the Upper Yangtze area. The results show that the $\delta^{13}C_{CH4}$, $\delta^{13}C_{C2H6}$, and $\delta^{13}C_{C3H8}$ of Longmaxi shale gas are all positively correlated with Ro. According to the distribution model of $\delta^{13}C$ with thermal maturity, the Longmaxi shale gas lies in the reversal stage. Shale gas is a mixture of the kerogen cracking gas and secondary cracking gas, and the mixing ratio of the two cracking gas can be estimated by isotopic fractionation experiments of thermogenic gas. The proportion of secondary cracking gas in the shale gas of the Longmaxi Formation ranges from 33 to 72%. The increase of secondary cracking gas with lower $\delta^{13}C$ would reduce the carbon isotope of the shale gas. The $\delta^{13}C_{C2H6}$ and $\delta^{13}C_{C3H8}$ have acute sensitivity to the occurrence of secondary cracking gas, hence they can be used as potential indicators of shale gas content. The decline of gas generation capacity, the reduction of micropores, and the destruction of tectonic movement are the considerable factors leading to the decrease of gas content in high-maturity shale.

Keywords: methane, isotopic reversal, gas content, secondary cracking, over-mature

INTRODUCTION

Organic alkane gas is a small molecule hydrocarbon formed by the degradation or cracking of organic matter under specific temperature, pressure, and catalytic conditions. As the principles of kinetic isotopic effect have been widely accepted, alkane carbon and hydrocarbon isotopic analysis has made remarkable achievements in studying the genesis and accumulation of natural gas (Berner et al., 1995; Cramer et al., 2001; Cramer, 2004; Burruss and Laughrey, 2010; Wang et al., 2015; Curiale and Curtis, 2016; Cao et al., 2020; Feng et al., 2020; Li et al., 2020). The carbon and hydrogen isotopes

composition of organic alkane gas is not only related to the material composition of the hydrocarbon generation material, but also effected by the isotope fractionation in the process of biochemical degradation or thermal evolution cracking (Burruss & Laughrey, 2010). In addition, they are also influenced by secondary changes during migration and accumulation after hydrocarbon generation. Therefore, they contain vast quantities of information on hydrocarbon accumulation (Cai et al., 2005; He, 2017).

Shale gas is formed in a relatively closed system characterized by self-generation, self-storage, and *in-situ* accumulation. Due to its wide distribution and tremendous resource, shale gas has become a vital natural gas resource globally (Curtis, 2002; Zou et al., 2010; Freeman et al., 2011; Huang et al., 2020a). Distinct from with the accumulation of conventional gas, the formation of shale gas lacks secondary migration. In addition, it is affected by the cracking of retained hydrocarbon and Rayleigh fractionation in the high- and over-mature stage, and desorption and fractionation of depressurization associated with tectonic uplift (Burruss and Laughrey, 2010; Tilley et al., 2011; Xia et al., 2013; Feng et al., 2020; Jiang et al., 2020; Milkov et al., 2020). Therefore, carbon and hydrogen isotopes of shale gas show distinct characteristics from those of conventional natural gas. The carbon isotopic reversals or rollovers of shale gas are common in the high- and over-mature shale gas, such as Fayetteville shale gas in North America and Longmaxi shale gas in Sichuan Basin, China (Tilley et al., 2011; Zumberge et al., 2012; Dai et al., 2014). However, there are no carbon isotopic reversals in low-mature shale gas, such as Eagle Ford Shale and Chang seven Shale in Ordos Basin (Dai et al., 2016; He, 2017). Moreover, the shale gas wells with carbon isotopic reversals tend to have high production, which has attracted significant attention. Considerable amount of researches have been carried out on the causes of carbon isotopic reversals in high- and over-mature shale gas. Currently, the main views on the cause of carbon isotopic reversals in high- and over-mature shale gas are as follows: the mixture of kerogen- and oil-cracking gases (Tilley and Muehlenbachs, 2013; Xia et al., 2013; Zhao et al., 2019), Rayleigh fractionation of alkanes (Burruss and Laughrey, 2010; Feng et al., 2020), carbon exchange at high temperature (Dai et al., 2016; Yang et al., 2017), Fischer-Tropsch synthesis (Tang and Xia, 2011); water-kerogen redox reaction (Price, 2001; Burruss and Laughrey, 2010), decomposition of C_{2+} alkanes (Telling et al., 2013; Xia and Gao., 2018), isotope fractionation during the desorption process (Freeman et al., 2011; Wang et al., 2015; Ma et al., 2020), isotope fractionation caused by tectonic uplift (Jiang et al., 2020; Milkov et al., 2020).

In recent years, China has vigorously developed unconventional oil and gas (Tang et al., 2015; Feng et al., 2018; Huang et al., 2020b, 2021), and achieved a yearly shale gas output of 200×10^8 m^3 in 2020, becoming the largest shale gas production country outside North America (Zou et al., 2021). Although China has made significant breakthroughs in marine shale gas and terrestrial shale gas, the current shale gas production mainly comes from the Ordovician Wufeng Formation shale and Silurian Longmaxi Formation shale (Longmaxi shale for short) in the Upper Yangtze area (Zhao et al., 2020). The Longmaxi shale is widely distributed in the Upper Yangtze area. Currently, the production of Longmaxi shale gas is mainly carried out in the Changning, Weiyuan, Zhaotong, Fuling and other blocks in the Sichuan Basin and the surrounding areas. There are still plenty of shale gas resources to be developed in the Upper Yangtze area.

Numerous studies on the carbon and hydrogen isotopes of Longmaxi shale gas in the Upper Yangtze area have been carried out, but these studies mainly focus on a single block (Tang et al., 2015; Yang et al., 2017; Feng et al., 2018; Chen et al., 2020). There are few studies comparing the isotopic composition of shale gas from different regions and its connection with gas content. We studied the data from 102 wells in eight shale gas production blocks in the Upper Yangtze area and compared their thermal maturity, gas content, composition, and isotopes composition of Longmaxi shale gas. The relationships between alkane carbon isotopes and thermal maturity, cracking gas composition, and gas content of shale gas are analyzed. Thus, some possible factors affecting the enrichment of Longmaxi Formation gas are discussed. We hope that this study will provide a reference for exploring the shale gases with high- or over-maturity.

GEOLOGICAL SET

The Upper Yangtze area mainly includes the Sichuan Basin, Chongqing Province, and the north of Guizhou Province and Yunnan Province (**Figure 1**). The Longmaxi shale is rich in graptolite fossils, which are mainly deposited in the marine shelf environment, and are characterized by high bio-silicon content and high TOC (Xu et al., 2004). The black shale of the Longmaxi Formation is continuous and thick, generally up to 300 m. The abundance of organic matter in Longmaxi shale is relatively high and gradually increases from top to bottom, with a TOC of 5.1–6.8%. High-quality shale reservoirs are mainly located at the bottom of the shale interval of 10–60 m and are the leading shale gas-producing layer (Dai et al., 2016; Yang et al., 2017; Zou et al., 2021). The burial depth of Longmaxi shale in the Upper Yangtze area is 500–6000 m. Commercial exploitation of shale has been fulfilled in the shale shallower than 3500 m. A breakthrough in production has been partially achieved in the deep shale of 3500–4500 m. The distribution area of shale below 4500 m is about 3.09×10^4 km^2, and the recoverable shale gas resource is estimated to be 3.78×10^{12} m^3, which shows good prospects for exploration (Zhao et al., 2020; Zou et al., 2021). The reservoir quality and gas-bearing properties of the Longmaxi shale in the Upper Yangtze area are obviously heterogeneous. The enrichment of shale gas is controlled by many factors such as organic matter abundance, thermal maturity, tectonic evolution, roof, floor thickness, structural morphology, and fault development (Ou et al., 2018; Jiang et al., 2020; Xi et al., 2022).

DATA SET

Table 1 lists the molecular composition and carbon and hydrogen isotopic data of eight major shale gas fields (i.e., Weiyuan,

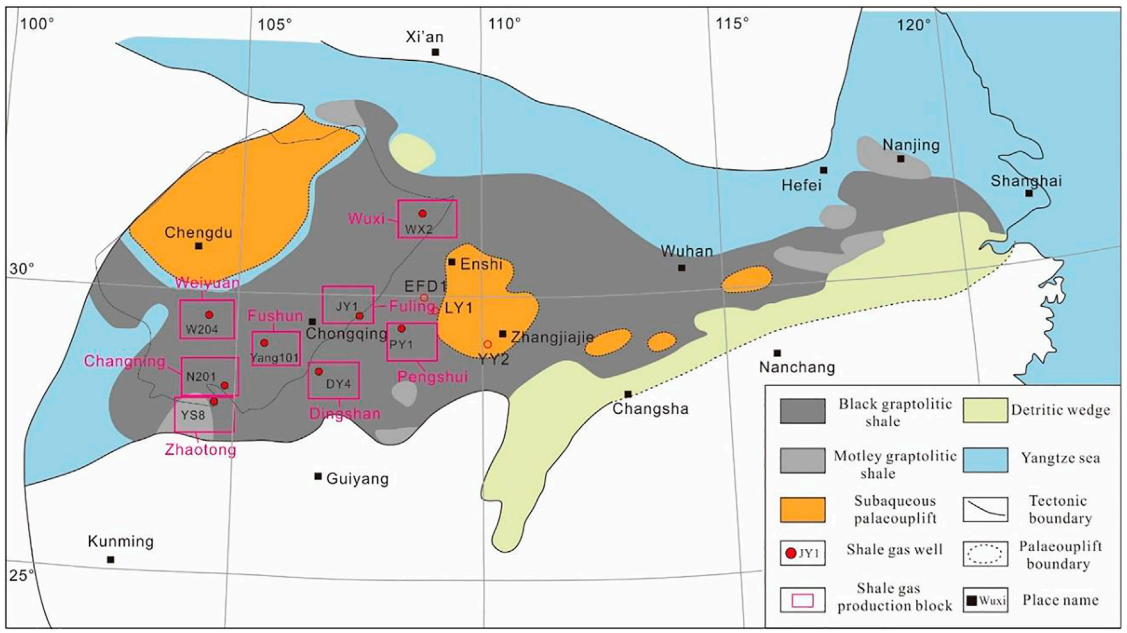

FIGURE 1 | Paleogeography of Longmaxi shale and distribution of main shale gas blocks in the Upper Yangtze area (modified from Xu et al., 2004).

TABLE 1 | Geochemical characteristics of shale gas from Longmaxi formation in the Upper Yangtze area (Data from Dai et al., 2014; 2016; 2017; Wu et al., 2015; 2017; Yang et al., 2017; Feng et al., 2018; 2019; Xin et al., 2019; Cao et al., 2020).

Shale gas block	Main component (mean, %)				Carbon and hydrogen isotopes (mean, ‰)				Numer of gas samples
	CH_4	C_2H_6	C_3H_8	Wetness	$\delta^{13}C_{CH4}$	$\delta^{13}C_{C2H6}$	$\delta^{13}C_{C3H8}$	δD_{CH4}	
Weiyuan	98.21	0.52	0.02	0.547	−35.08	−39.49	−41.44	−6.42	28
Changning	98.44	0.37	0.01	0.385	−27.96	−34.31	−36.28	−5.33	18
Zhaotong	98.98	0.45	0.02	0.473	−27.58	−33.1	−35.08	2.5	16
Fushun	97.57	0.42	0.02	0.449	−33.48	−35.23	−39.4	0.1	6
Dingshan	98.43	0.58	0.01	0.596	−30.69	−34.12	−37.43	0.23	2
Fuling	98.55	0.67	0.03	0.705	−30.54	−35.51	−39.09	5.32	27
Pengshui	98.62	0.63	0.01	0.645	−30.13	−34.23	−47.45	3.2	3
Wuxi	94.54	0.26	-	0.274	−29.3	−31.65	-	-	2

Changning, Zhaotong, Fushun, Dingshan, Jiaoshiba, Pengshui, Wuxi) in the Upper Yangtze area (Dai et al., 2014, 2016, 2017; Wu et al., 2015, 2017; Yang et al., 2017; Feng et al., 2018, 2019; Xin et al., 2019; Cao et al., 2020). There are usually some differences in the stable isotopes of gases obtained by different sampling means. Numerous desorption experiments show that the desorption rate of methane in shale is significantly faster than that of ethane and propane. In addition, alkanes enriched in 12C are more accessible to release from shale than alkanes enriched in 13C (Wang et al., 2015; Liu et al., 2018; Ma et al., 2020). Therefore, the data analyzed in this study are all gas samples collected at the wellhead. Some wells are sampled multiple times, and only the latest data are used in this study. The latest data after stable production tend to be more accurate, and the molecular and isotopic compositions of shale gas would change little after a short period of production (Zhang et al., 2018). The primary geological characteristics, such as static (depth, thickness, thermal maturity, porosity, brittleness) and dynamic parameters (gas content, and pressure cofficient) of Longmaxi shale from different blocks, were also collected. Although the Longmaxi shale is thick, the shale gas is mostly from high-quality shale reservoirs at the bottom of the shale intervals. The static parameters of shale gas wells are mainly the average values of high-quality shale reservoirs. **Table 2** shows no momentous distinction among the static parameters of shale, but the dynamic parameters show significant differences. In particular, the gas content showed obvious differences, distributed between 0.45 and 8.0 m^3/t.

The Longmaxi Shale gas is mainly dominated by methane with a wetness of less than 5%, which shows the characteristics of dry gas at the over-mature stage. The carbon and hydrogen isotopes of Longmaxi shale gas in the eight shale gas blocks are quite different. Longmaxi shale gas has $\delta^{13}C_{CH4}$ values from −26.3‰ to −37.3‰, $\delta^{13}C_{C2H6}$ values from -31.0‰ to −42.8‰, $\delta^{13}C_{C3H8}$ values from −33.1‰ to −50.5‰, and δD_{CH4} values from -129‰ to −163‰. Among them, the carbon and hydrogen isotopes of Longmaxi shale gas in the Weiyuan block are relatively low, while

TABLE 2 | Primary geological characteristics of Longmaxi formation shale in the Upper Yangtze area (Data from Dong et al., 2016; Zou et al., 2016; Zhao et al., 2020).

Shale gas block	Depth (m)	Thickness of high-quality shale (m)	TOC (%)	Ro (%)	Porosity (%)	Brittleness in dex	Gas content (m^3/t)	Formation pressure coefficient
Weiyuan	2000–3,700	30–60	1.0–10.2	1.8–2.45	1.7–10.9	42–96	2.3–7.5	1.4–2.0
Changning	1,500–1,600	60–80	1.9–7.3	2.3–3.15	3.4–8.4	42–95	3.1–7.8	1.3–2.0
Zhaotong	2,390–2,516	30–40	2.1–6.0	2.5–3.25	3.4–7.4	55–63	2.4–4.5	1.05–1.96
Fushun	3,200–4,500	80	3.0–4.0	2.8–3.0	3.5–4.5	>50	3.5–4.2	
Dingshan	2,240–3,780	28–32	3.0–3.5	2.0–2.66	3.0–5.9	60–70	2.0–6.6	0.98–1.85
Fuling	2000–4,000	40–80	1.5–6.1	2.2–3.1	3.7–8.1	50–80	1.3–6.3	1.55
Pengshui	2,500–3,000	40–80	1.0–3.0	2.5–4.4	0.2–2.28	44–66	0.45–2.46	
Wuxi	1,500–2000	26–70	3.0–11.0	2.0–3.49	3.0–6.0	>50	2.5–8.0	>1.2

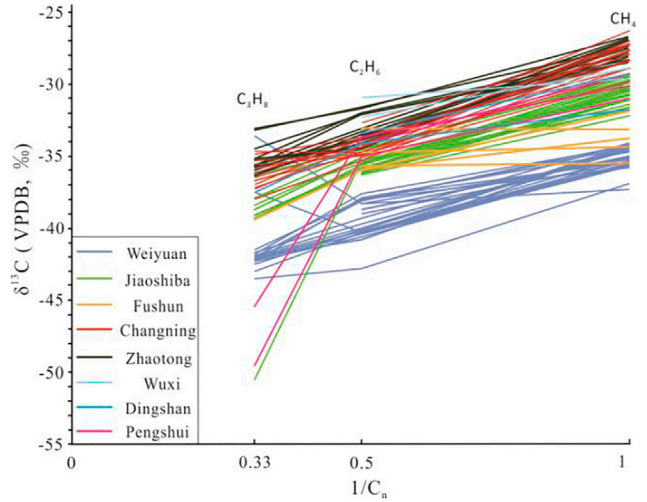

FIGURE 2 | Carbon isotopes distribution of Longmaxi shale gas in the Upper Yangtze area.

those of Longmaxi shale gas in the Zhaotong block are relatively high. In addition, the shale gases in eight blocks all show the characteristics of complete carbon isotope reversal ($\delta^{13}C_{CH4} > \delta^{13}C_{C2H6} > \delta^{13}C_{C3H8}$) (**Figure 2**). The shale gas in the Changning block has the most significent carbon isotope reversal, with an average $\delta^{13}C_{CH4}-\delta^{13}C_{C2H6}$ of 6.34‰, while the shale gas in the Fushun block has the smallest carbon isotope reversal, with an average $\delta^{13}C_{CH4}-\delta^{13}C_{C2H6}$ of 1.75‰. These indicate that the geological conditions of different blocks may have an essential influence on the isotope characteristics of the Longmaxi shale gas.

DISCUSSION

The Origin of Longmaxi Shale Gas

The isotope characteristics of alkane gas are a standard method for identifying the source of natural gas, and has achieved good results in the exploration of conventional gas and coalbed methane (Berner et al., 1995; Cramer et al., 2001; Cramer, 2004; Burruss & Laughrey, 2010; Telling et al., 2013). It is generally considered that the carbon isotope of organic methane is less than −25‰, while that of inorganic methane is greater than −25‰ (Jenden et al., 1993). As shown in **Table 1**, $\delta^{13}C_{CH4}$ of Longmaxi shale gas in the Upper Yangtze area are all less than −25‰, indicating organic origin. Whiticar, 1999 established a $\delta^{13}C_{CH4}-\delta D_{CH4}$ diagram based on the study of methane from various recent and ancient sedimentary environments to distinguish natural gas of different sources. As shown in **Figure 3**, the Longmaxi shale gas is located in the organic high-mature origin area.

However, not all isotopic-based identification methods of natural gas genesis are still applicable to high- and over-mature shale gas reservoirs. For instance, the Bernard diagram modified by Chen et al. (1995), which is widely used in conventional gas, are no longer accurate in identifying the genesis of shale gas. As shown in **Figure 4A**, Longmaxi shale gases partly fall in the oil cracking gas category and partly in the mixed area of inorganic gas and coal-derived gas. It is contradictory that the original organic matter of Longmaxi shale was dominated by the type I or type II_1 kerogen (Ou et al., 2018; Jiang et al., 2020). The discrimination diagram of $\delta^{13}C_{CH4}$-$\delta^{13}C_{C2H6}$-$\delta^{13}C_{C3H8}$ (Dai, 1992) is also not applicable to Longmaxi shale gas. As shown in **Figure 4B**, most Longmaxi shale gases fall outside the indicator areas. Especially in the $\delta^{13}C_{CH4}$-$\delta^{13}C_{C3H8}$ map, almost all shale gas is not in the indicator zone, indicating that shale gas is different from the organic nature gas seen in the past. Distinct with the conventional gas originating from marine sapropel organic matter (Dai et al., 2014), the $\delta^{13}C_{CH4}$ of Longmaxi shale gases are higher. Meanwhile, the $\delta^{13}C_{C2H6}$ of and $\delta^{13}C_{C3H8}$ of Longmaxi shale gas are dramatically lower. Therefore, some new indicators or genetic maps are needed to identify the origin of shale gas. Milkov and Etiope (2018) modified several genetic diagrams based on the data of 20,000 natural gas samples worldwide. As shown in **Figure 5**, the 1Longmaxi shale gas belongs to late-mature thermogenic gas.

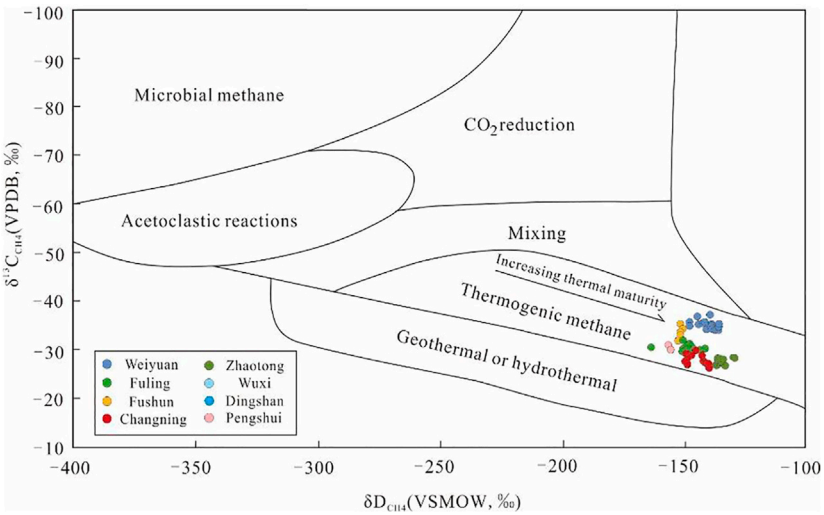

FIGURE 3 | Plot of $\delta^{13}C_{CH4}$–δD_{CH4} for identification of genetic types of Longmaxi shale gas in the Upper Yangtze area (modified from Whiticar, 1999).

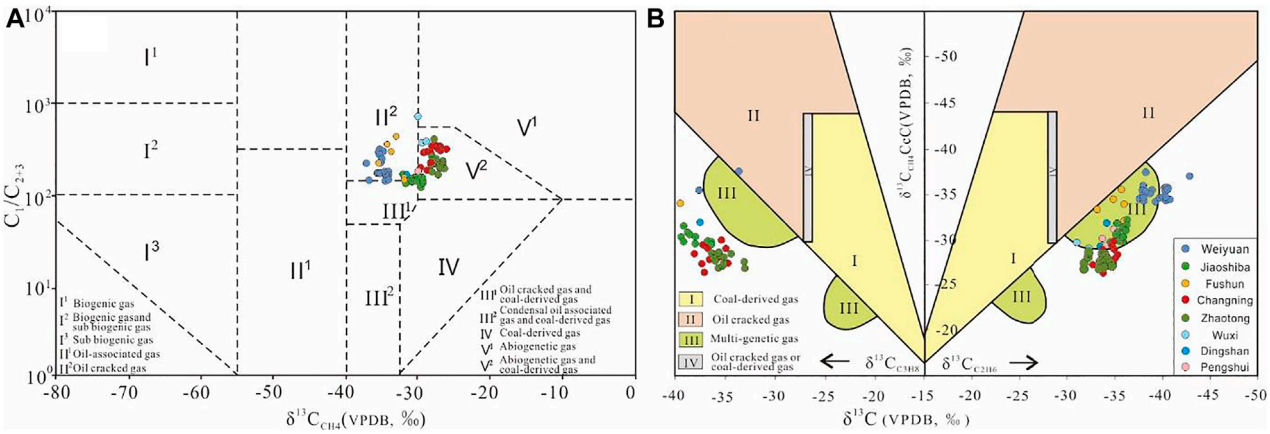

FIGURE 4 | Discrimination diagram of gas origin for Longmaxi shale gas in the Upper Yangtze area. **(A)** Modified Bernard diagram about the relationship between $\delta^{13}C$ and $C_1/(C_2 + C_3)$, base map from reference (Chen et al., 1995); **(B)** relationship between $\delta^{13}C_{CH4}$, $\delta^{13}C_{C2H6}$, and $\delta^{13}C_{C3H8}$, base map from reference (Dai et al., 2014; Liu et al., 2016).

Cracking Gas Composition of Longmaxi Shale Gas

It is gradually accepted that the retained crude oil and wet gas in the shale would crack and generate considerable amounts of secondary cracking gas during the high- and over-mature stages (Zhao et al., 2019). Based on the humidity and alkane carbon isotopes of shale gas with different thermal maturities globally, previous studies show that the carbon isotopes of shale gas changes in an inverted "S" shape with the decrease in the humidity (Tilley et al., 2011; Zumberge et al., 2012; Hao and Zou, 2013). As we all know, natural gas humidity decreases with thermal maturity. As the thermal maturity of shale increases, the carbon isotope composition of shale gas will undergo several stages of change from normal isotope sequence to partial reversal isotope sequence and complete reversal isotope sequence (Tilley and Muehlenbachs, 2013; Dai et al., 2014). Xia et al. (2013) proposed a distribution model of alkane carbon isotopes of shale gas with increasing thermal maturity and divided it into four stages (I, II, III, and IV) according to the characteristics of carbon isotope (**Figure 6A**).

Figure 6B shows the relationship between the alkane carbon isotopes of the Longmaxi shale gas and the thermal maturity. The $\delta^{13}C_{CH4}$, $\delta^{13}C_{C2H6}$, and $\delta^{13}C_{C3H8}$ of Longmaxi shale gas all increase with Ro. The increase rate of $\delta^{13}C_{C2H6}$ and $\delta^{13}C_{C3H8}$ is greater than that of $\delta^{13}C_{CH4}$. It is consistent with stage III in the model proposed by Xia et al. (2013). At stage III, the cracking of retained hydrocarbon in the shale reaches a peak and begins to decrease gradually. Previous studies suggested that the isotope fractionation of secondary cracking is more potent than that of kerogen cracking, so the alkane carbon isotopes of secondary

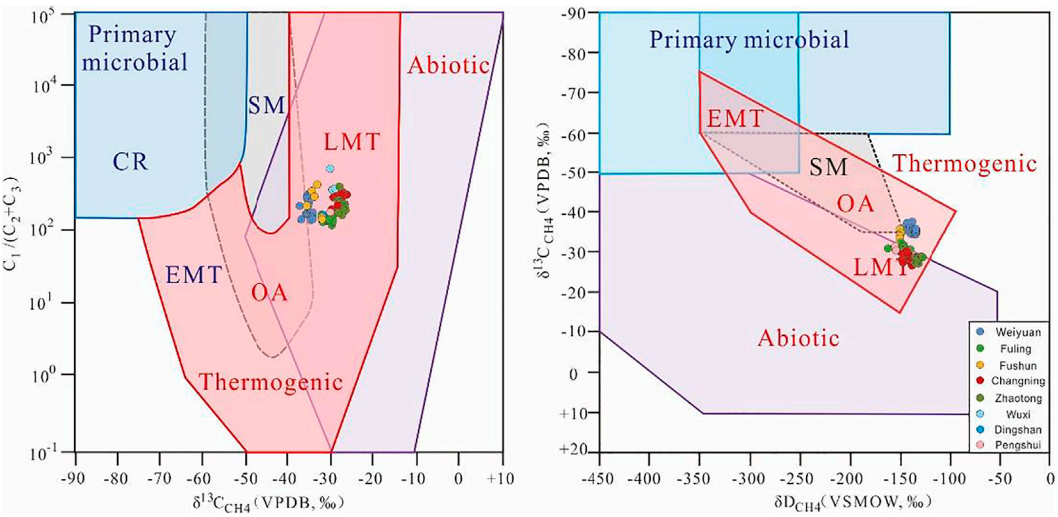

FIGURE 5 | Genetic diagram of nature gas revised by Milkov and Etiope (2018). CO_2 reduction (CR), methyl-type fermentation (F), secondary microbial (SM), early mature thermogenic gas (EMT), oil-associated (mid-mature) thermogenic gas (OA), and late-mature thermogenic gas (LMT).

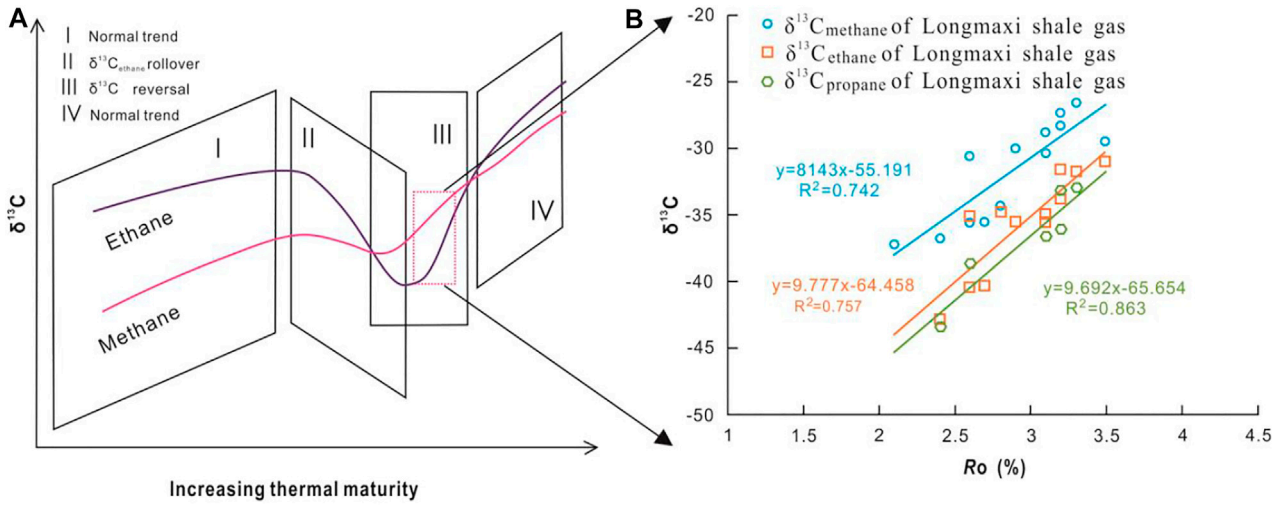

FIGURE 6 | (A) Distribution mode of $\delta^{13}C$ with thermal maturity proposed by Xia et al. (2013). **(B)** Relationship between the $\delta^{13}C$ and *Ro* of Longmaxi shale gas in the Upper Yangtze area.

cracking gas are lighter than those of kerogen cracking gas (Tilley et al., 2011; Hao and Zou, 2013; Xia et al., 2013; Zhao et al., 2019). Therefore, as the secondary cracking of the over-mature shale weakens, the alkane carbon isotopes of shale gas gradually increases. Ethane and propane are low in shale gas, so $\delta^{13}C_{C2H6}$ and $\delta^{13}C_{C3H8}$ are more sensitive to $\delta^{13}C_{CH4}$. The trend lines of $\delta^{13}C_{C2H6}$ and $\delta^{13}C_{C3H8}$ show a more significant slope than that of $\delta^{13}C_{CH4}$, as shown in **Figure 6B**. When *Ro* increases to around 4%, the $\delta^{13}C_{C2H6}$ and $\delta^{13}C_{C3H8}$ will be greater than that of $\delta^{13}C_{CH4}$, and the carbon isotope of shale gas will eventually return to a positive order. Liu et al. (2018) studied the extremely high mature shale gas in Southern North China Basin and found that the carbon isotope composition of shale gas with *Ro* ≈ 4.1% shows a normal sequence.

There is a large amount of retained oil and wet gas in organic-rich shale at the mature stage. When the thermal maturity reaches a certain level (such as *Ro*>1.6%), the retained hydrocarbon begins to crack and generate gas. At this time, there are both kerogen cracking gas and secondary cracking gas in the shale. The carbon and hydrogen isotopes of methane in the kerogen cracking gas and the secondary cracking gas are different. Therefore, it can be used to analyze the composition of kerogen cracking gas and secondary cracking gas in shale gas (Li et al., 2020). According to the isotope fractionation

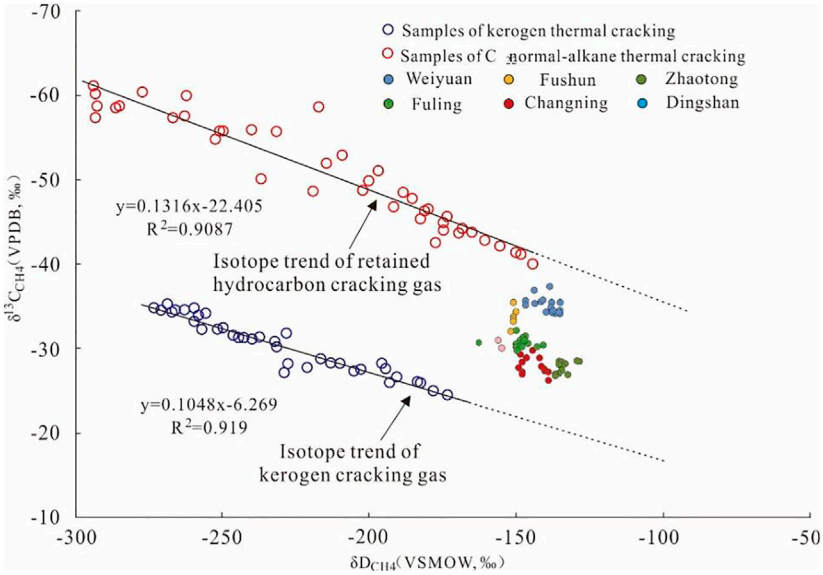

FIGURE 7 | Relationship between methane carbon and hydrogen isotopes of thermal simulation results of kerogen and nC22 (modified from Qu 2015).

mechanism of thermogenic gas (Berner et al., 1995; Cramer et al., 2001), comparative experiments on the thermal cracking of kerogen and normal C_{22} alkanes (retained liquid hydrocarbon equivalent) have been carried out. The trend models of $\delta^{13}C_{CH4}$ and δD_{CH4} for two types of cracking gas are established (Qu, 2015). **Figure 7** shows that Longmaxi shale gas is located in the middle of the trend lines of kerogen cracking gas and secondary cracking gas. It is consistent with the previous research that shale gas is a mixture of kerogen cracking gas and secondary cracking gas (Tilley et al., 2011; Hao and Zou, 2013; Xia et al., 2013; Yang et al., 2017; Zhao et al., 2019; Milkov et al., 2020).

Therefore, the cracking gas composition of shale gas can calculate based on this research. The vertical line based on the hydrogen isotope of Longmaxi shale gas ($\delta D_{CH4\text{-}shale}$) will intersect with the extension of the $\delta^{13}C_{CH4}$-δD_{CH4} trend line of kerogen cracking gas and retained hydrocarbon cracking gas (**Figure 7**). The two intersection points respectively represent the $\delta^{13}C_{CH4}$ of the kerogen cracking gas and secondary cracking gas. They can be expressed as $\delta^{13}C_{CH4\text{-}kero}$ and $\delta^{13}C_{CH4\text{-}seco}$ (**Eqs 1**, **2**). The methane carbon isotope of Longmaxi shale gas ($\delta^{13}C_{CH4\text{-}shale}$) is a mixture of two end members. Therefore, the equation of $\delta^{13}C_{CH4\text{-}shale}$, $\delta^{13}C_{CH4\text{-}kero}$, and $\delta^{13}C_{CH4\text{-}seco}$ can be established. The ratio of retained hydrocarbon cracking gas is X, while that of kerogen cracking gas is 1-X (**Eq. 3**).

$$\delta^{13}C_{CH4-kero} = 0.1048*\delta D_{CH4-shale} - 6.269 \quad (1)$$

$$\delta^{13}C_{CH4-seco} = 0.1316*\delta D_{CH4-shale} - 22.405 \quad (2)$$

$$\delta^{13}C_{CH4-shale} = (1 - X)*\delta^{13}C_{CH4-kero} + X*\delta^{13}C_{CH4-seco} \quad (3)$$

When the $\delta^{13}C_{CH4\text{-}shale}$ and $\delta D_{CH4\text{-}shale}$ of shale gas samples are substituted into the above equations, the ratio of kerogen cracking gas and retained hydrocarbon cracking gas can be obtained.

The proportion of retained hydrocarbon cracking gas in the Longmaxi shale gas ranges from 31 to 83% (**Table 3**). Among the six shale gas blocks (no $\delta D_{CH4\text{-}shale}$ in the Wuxi and Dingshan blocks), the proportion of retained hydrocarbon cracking gas in the Weiyuan block is the highest (average 72%), while that in the Changning block is the lowest (average 33%). There are two possible causes for the difference in the composition of cracking gas in shale gas. 1) The thermal maturity of Longmaxi shale in the Weiyuan block (*Ro* of 2.1–2.7%) is lower than that in other shale gas blocks, and it is still in the stage of retained hydrocarbon cracking. However, the thermal maturity of Longmaxi shale in the Changning block is exceptionally high (*Ro* of 3.1–3.2%). Most retained hydrocarbons of Longmaxi shale in the Changning block have been consumed, resulting in a reduction of secondary cracking gas. Therefore, the proportion of secondary cracking gas in the Weiyuan block is higher than that in the Changning block. 2) As the Weiyuan block is close to the Leshan-Longnüsi paleo-uplift, its preservation conditions are relatively poor. Liu et al. (2016) believed that there is communication between the Weiyuan anticline and the surface, which accounts for the low pressure of Longmaxi shale gas in the Weiyuan block. The shale gas generated in the early stage may dramatically dissipate during the tectonic uplift. Thus, the secondary cracking gas primarily developed in the later period plays an essential contribution to the shale gas.

Implication of Carbon Isotopes for Shale Gas Content

Gas content is the focus of shale gas resource evaluation. Previous studies suggest that the shale gas wells with carbon isotope reversal tend to be highly productive (Tilley et al., 2011; Zumberge et al., 2012). Feng et al. (2018) believed that the daily output of Longmaxi shale gas wells in the Weiyuan block shows

TABLE 3 | Proportion of kerogen cracking gas and secondary cracking gas in Longmaxi shale gas in the Upper Yangtze Area.

Block	$\delta^{13}C_{CH4\text{-}shale}$ (‰)	$\delta D_{CH4\text{-}shale}$ (‰)	$\delta^{13}C_{CH4\text{-}kero}$ (‰)	$\delta^{13}C_{CH4\text{-}seco}$ (‰)	Proportion of secondary gas (%)
Weiyuan	–37.3~–34.1 (-35.08)	–135~–147 (–138)	–21.7~–20.4 (–20.8)	–41.8~–40.2 (–40.7)	67–83 (72)
Changning	–26.3~–29.8 (–28.0)	–149~–139 (–145)	–21.9~–20.9 (–21.4)	–42.0~–40.7 (–41.4)	26–42 (33)
Zhaotong	–28.5~–26.8 (–27.7)	–137~–129 (–134)	–20.6~–19.8 (–20.4)	–40.4~–39.4 (–40.1)	31–44 (37)
Fushun	–35.5~–32.0 (–33.5)	–152~–150 (–151)	–22.2~–22.0 (–22.1)	–42.4~–41.2 –42.3)	48–66 (58)
Fuling	–32.2~–29.4 (–30.5)	–163~–141 (–148)	–23.4~–21.1 (–21.9)	–43.8~–41.0 (–42.0)	36–51 (44)
Pengshui	–31.0~–29.3 (–30.5)	–156~–155 (–156)	–22.6~–22.5 (–21.6)	–42.9~–42.8 (–42.9)	37–41 (39)

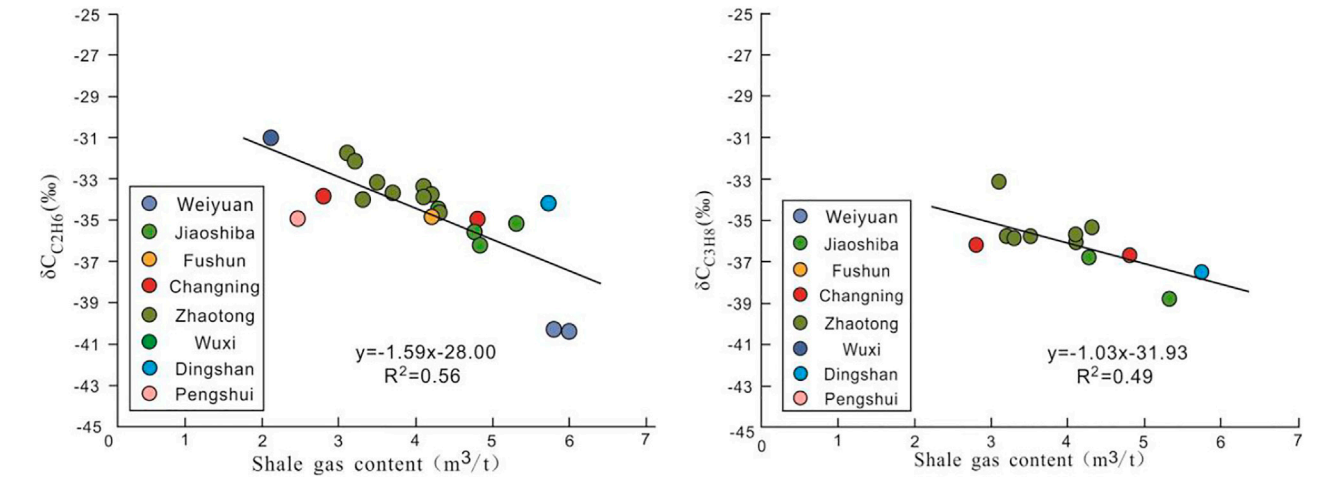

FIGURE 8 | Plots of $\delta^{13}C_{C2H6}$ and $\delta^{13}C_{C3H8}$ versus gas content of Longmaxi shale gas in the Upper Yangtze Area.

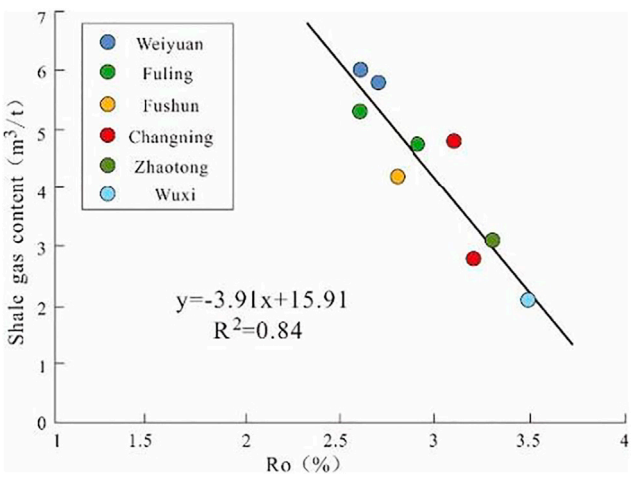

FIGURE 9 | Relationship between *Ro* and gas content of Longmaxi shale gas in the Upper Yangtze Area.

a positive relationship with the magnitude of carbon isotope reversal ($\delta^{13}C_{CH4}$-$\delta^{13}C_{C2H6}$). Chen et al. (2020) proposed that the gas content of Longmaxi shale in the Zhaotong block was positively correlated with $\delta^{13}C_{CH4}$-$\delta^{13}C_{C2H6}$ and negatively correlated with $\delta^{13}C_{C2H6}$. **Figure 8** shows the correlations between the gas content and carbon isotopes of Longmaxi shale gas in the Upper Yangtze area. The shale gas content exhibits a moderate correlation with $\delta^{13}C_{C2H6}$ and $\delta^{13}C_{C3H8}$. As the shale gas content increases, the $\delta^{13}C_{C2H6}$ and $\delta^{13}C_{C3H8}$ become lighter.

The $\delta^{13}C_{C2H6}$ and $\delta^{13}C_{C3H8}$ of Longmaxi shale gas are positively correlated with thermal maturity and negatively correlated with gas content. It means that the gas content of Longmaxi shale may decrease with thermal maturity. It can also be drawn from the relationship between thermal maturity and gas content of Longmaxi shale in the Upper Yangtze area (**Figure 9**). However, this is inconsistent with previous studies that the shale gas content increases with thermal maturity (Zou et al., 2010; Liu et al., 2016).

The shale gas content shows distinct variation characteristics at different maturity stages (**Figure 10**). The gas content of shale increases with the thermal maturity during the relatively low mature stage (*Ro*<2.2–2.6%). The gas content of shale decreases with the thermal maturity during the relatively high mature stage (*Ro*>2.2–2.6%). Our observations suggest that the following causes may lead to the decrease of Longmaxi shale gas content with thermal maturity.

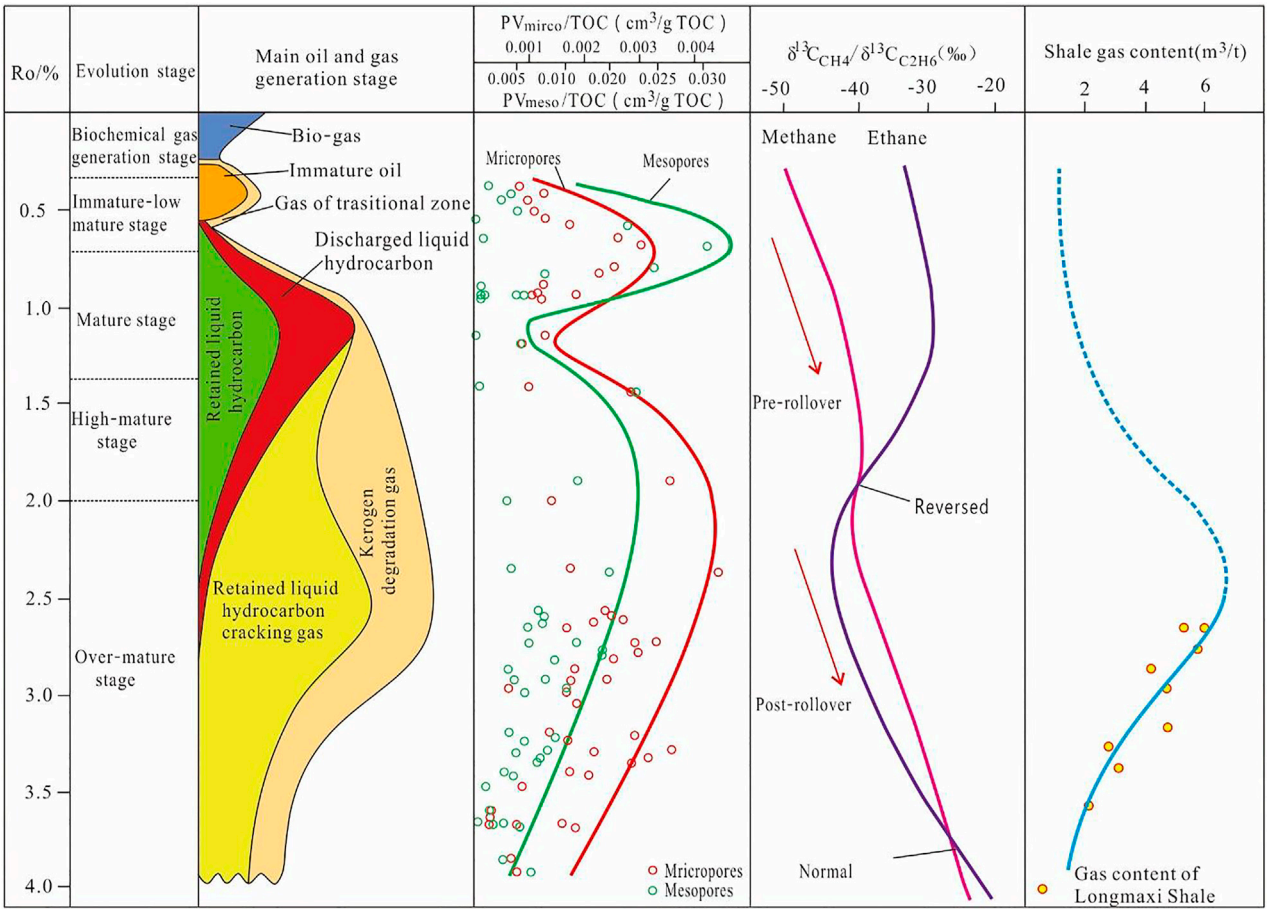

FIGURE 10 | Schematic diagram for hydrocarbon generation, pore volume, alkane carbon isotopes, and gas content at different mature stages in shales (modified from Li et al., 2018; Wang et al., 2019; Liu et al., 2018).

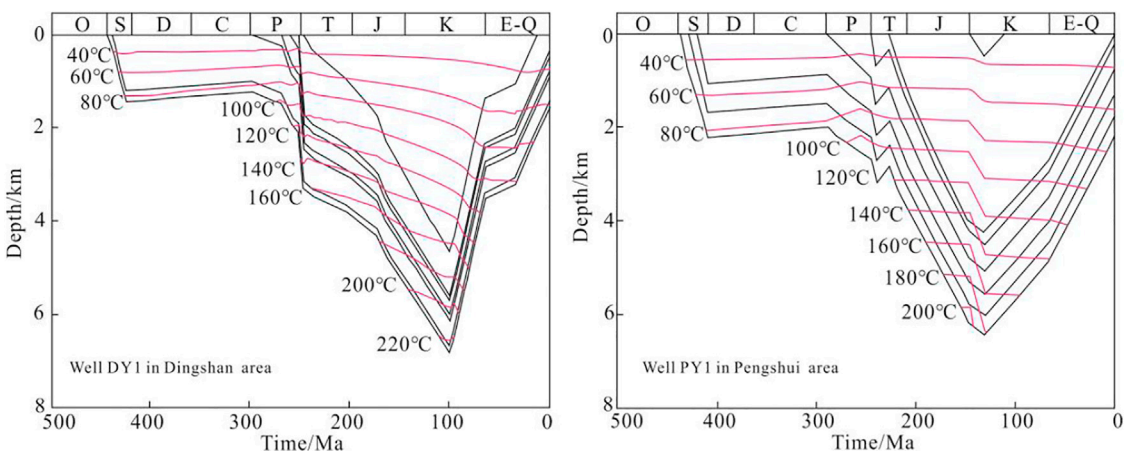

FIGURE 11 | Comparison of the burial histories of well DY1 in Dingshan block and well PY1 in Pengshui block (modified from Xu et al., 2015 and Qiu et al., 2020).

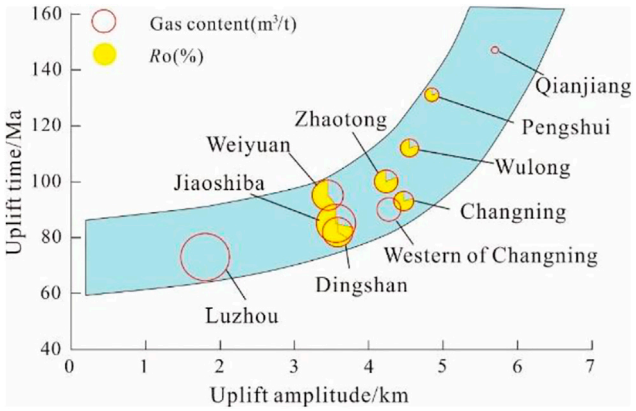

FIGURE 12 | connection among gas content, *R*o, uplift time, and uplift amplitude of Longmaxi shale gas in Yangtze Area (modified from Jiang et al., 2020). The size of the red circle represents the level of air content.

1) The consumption of organic matter in high- and over-mature shale leads to a significant decline in gas generation capacity, which may be an essential factor in the reduction in shale gas content. It has been suggested that hydrocarbon generation always exists in the source rocks with the thermal maturity (*R*o) less than 5% (Li et al., 2018). The hydrocarbon generation process of organic matter can be divided into five periods, including biochemical gas generation (0% < *R*o <0.3%), low maturity (0.3% < *R*o <0.7%), mature (0.7% < *R*o <1.3%), high-mature (1.3% < *R*o <2.0%), over-mature (2.0% < *R*o <5.0%). The products of hydrocarbon generation mainly include biogas, immature oil and transition gas, mature crude oil and associated gas, kerogen degradation gas, liquid hydrocarbon cracking gas, wet gas cracking gas, and methane cracking gas. Kerogen cracking gas is mainly produced when *R*o>1.1% and reaches the peak when Ro ≈ 1.6%, then gradually exhausts and stops when *R*o ≈ 3.0% (Chen et al., 2007; Jiang et al., 2020). Liquid hydrocarbons and wet gas are mostly cracking when *R*o>1.3%, and reach the peak when *R*o ≈ 2.6%, then gradually decrease and stop when *R*o ≈ 3.5% (Waples, 2000; Zhao et al., 2011; Li et al., 2018). Methane starts to crack when *R*o>5%. Therefore, high- and over-mature shale gas comprises kerogen cracking gas and secondary cracking gas. The Ro of the Longmaxi shale in the Upper Yangtze area is more significant than 2.0%, and in some blocks greater than 3.0%. Thus, the gas generation capacity of Longmaxi shale has been dramatically weakened.

2) The reduction of organic pores in over-mature shale may be another important factor leading to the decrease of gas content. Numerous micro-pores and nano-pores are generally developed in organic-rich shale (Loucks et al., 2012; Guo et al., 2017; Hu et al., 2017). These pores are mainly composed of organic pores and inorganic mineral matrix pores. The organic pores account for more than 50% of the storage space of shale (Singh et al., 2009; Passey et al., 2010). The content, type, and maturity of organic matter control the development of organic matter pores (Xu et al., 2019). Wang et al. (2019) established the pore structure evolution from immature shale to over-mature shale based on shale data worldwide. They proposed that the evolution of micropores and mesopores in shale could be divided into four stages. In the first stage (0.4% < *R*o <0.7%), the pore evolution is mainly related to the burial and compaction process. The discharge of liquid hydrocarbons generated by kerogen and the chemical dissolution of minerals would increase the pore volume (Loucks et al., 2012 ; ; Ko et al., 2018). In the second stage (0.7% < *R*o <1.2%), the filling of petroleum and bitumen leads to a significant reduction of pore volume in shale (Guo et al., 2017). In the third stage (1.2% < *R*o <2.2%), the micro-pores in the organic matter are significantly increased due to the secondary cracking of retained liquid hydrocarbons (Kuila et al., 2014; Hu et al., 2017). The matrix pores formed by inorganic minerals are gradually reduced due to compaction and cementation (Wang et al., 2013). In the fourth stage (*R*o>2.2%), the pores of organic matter in the shale begin to reduce significantly due to long-term compaction and graphitization of organic matter (Topór et al., 2017). The *R*o of the Longmaxi shale in the Lower Yangtze area is generally greater than 2.2%, and thus the reduction of micro-pores in the shale would decrease the gas content.

3) Tectonic movement affects the accumulation and destruction of shale gas. The time, amplitude, and scale of the last tectonic uplift have an essential impact on the differential enrichment of shale gas (Jiang et al., 2020). As seen in **Figure 11**, the amplitudes of last structure uplift in well DY1 and PY1 have slight difference, while the time of last structure uplift in well DY1 is significantly later than that in well PY1. When the shale reaches high- and over-maturity through deep burial, the gas escape in the shale will generally occur during the subsequent tectonic uplift and depressurization (Milkov et al., 2020). The time and amplitude of the last structure uplift will directly affect the shale gas content. The Longmaxi shale with higher thermal maturity tends to have an earlier period and greater amplitude of the last tectonic uplift. The last tectonic uplift is generally inclined to cause a decrease in gas content. Jiang et al. (2020) proposed the relationship between the gas content of the Longmaxi shale in the Yangtze area and the time and amplitude of the last tectonic uplift (**Figure 12**). There is a particular connection between the shale gas content and the last tectonic uplift. The shale gas content decreases with the enlargement of the uplift amount and the advance of the uplift period. On the contrary, it increases with the diminution of the uplift amount and the delay of the uplift period.

The completeness of the yellow circle represents the *R*o, and the full circle refers to Ro = 4%.

CONCLUSION

1) The alkane carbon and hydrogen isotopes of Longmaxi shale gas in the Upper Yangtze area are quite different. The isotopic characteristics and their differences are significant for the origin and accumulation of shale gas.
2) The high- and over-mature shale gas comprises kerogen cracking gas and secondary cracking gas. The proportion of secondary cracking gas in the Longmaxi shale gas is 33–72%. The carbon isotopes of shale gas gradually decrease with the content of secondary cracking gas.
3) The weakening of gas generation capacity and the reduction of micro-pores are essential reasons for the decrease of gas content in over-mature shale with thermal maturity. The

Longmaxi shale with higher thermal maturity tends to have an earlier period and greater amplitude of last tectonic uplift, which may be another cause of the decrease in gas content.

DATA AVAILABILITY STATEMENT

The raw data supporting the conclusions of this article will be made available by the authors, without undue reservation.

AUTHOR CONTRIBUTIONS

ZC: conception, database, statistical analysis, the first draft of the manuscript YL: database, statistical analysis LL: conception, statistical analysis LC: conception, design of the study, the first draft of the manuscript PW: statistical analysis YZ: database ZR: design of the study LJ: statistical analysis WD: database All authors contributed to manuscript revision, read, and approved the submitted version.

FUNDING

This research was supported by the Open Fund (PLC20210204) of State Key Laboratory of Oil and Gas Reservoir Geology and Exploitation (Chengdu University of Technology), the National Natural Science Foundation of China (42102177), the Natural Science Foundation of Shanxi Province of China (2021JQ-592), and the Foundation of Shaanxi Educational Committee (21JK0840).

ACKNOWLEDGMENTS

We would like to thank the PetroChina Zhejiang Oilfield Company for providing part of research data for this study.

REFERENCES

Berner, U., Faber, E., Scheeder, G., and Panten, D. (1995). Primary Cracking of Algal and Landplant Kerogens: Kinetic Models of Isotope Variations in Methane, Ethane and Propane. *Chem. Geology.* 126, 233–245. doi:10.1016/0009-2541(95)00120-4

Burruss, R. C., and Laughrey, C. D. (2010). Carbon and Hydrogen Isotopic Reversals in Deep basin Gas: Evidence for Limits to the Stability of Hydrocarbons. *Org. Geochem.* 41, 1285–1296. doi:10.1016/j.orggeochem.2010.09.008

Cai, C., Hu, G., He, H., Li, J., Li, J., and Wu, Y. (2005). Geochemical Characteristics and Origin of Natural Gas and Thermochemical Sulphate Reduction in Ordovician Carbonates in the Ordos Basin, China. *J. Pet. Sci. Eng.* 48 (3-4), 209–226. doi:10.1016/j.petrol.2005.06.007

Cao, C., Zhang, M., Li, L., Wang, Y., Li, Z., Du, L., Holland, G., and Zhou, Z. (2020). Tracing the Sources and Evolution Processes of Shale Gas by Coupling Stable (C, H) and noble Gas Isotopic Compositions: Cases from Weiyuan and Changning in Sichuan Basin, China. *J. Nat. Gas Sci. Eng.* 78, 103304. doi:10.1016/j.jngse.2020.103304

Chen, H. H., Sun, Y. C., and Sun, Q. M. (1995). Application of the δ13 Rayleigh Fractional Model to Determine the Processes of Gas Migration and Accumulation. *Pet. Explor Dev.* 22 (2), 29–33. **(in Chinese with English abstract)**.

Chen, J., Zhao, W., Wang, Z., Zhang, S., Deng, C., Sun, Y., et al. (2007). The Upper Maturity Limit and Potential of Gas Generation: A Case Study on marine Kerogen of Tarim Basin. *Chin. Sci. Bull.* 52 (S1), 95–99. doi:10.1007/s11434-007-6015-7

Chen, Z., Chen, L., Wang, G., Zou, C., Jiang, S., Si, Z., et al. (2020). Applying Isotopic Geochemical Proxy for Gas Content Prediction of Longmaxi Shale in the Sichuan Basin, China. *Mar. Pet. Geology.* 116, 104329. doi:10.1016/j.marpetgeo.2020.104329

Cramer, B., Faber, E., Gerling, P., and Krooss, B. M. (2001). Reaction Kinetics of Stable Carbon Isotopes in Natural GasInsights from Dry, Open System Pyrolysis Experiments. *Energy Fuels* 15 (3), 517–532. doi:10.1021/ef000086h

Cramer, B. (2004). Methane Generation from Coal during Open System Pyrolysis Investigated by Isotope Specific, Gaussian Distributed Reaction Kinetics. *Org. Geochem.* 35 (4), 379–392. doi:10.1016/j.orggeochem.2004.01.004

Curiale, J. A., and Curtis, J. B. (2016). Organic Geochemical Applications to the Exploration for Source-Rock Reservoirs - A Review. *J. Unconventional Oil Gas Resour.* 13, 1–31. doi:10.1016/j.juogr.2015.10.001

Curtis, J. B. (2002). Fractured Shale-Gas Systems. *AAPG Bull.* 86 (11), 1921–1938. doi:10.1306/61eeddbe-173e-11d7-8645000102c1865d

Dai, J., Ni, Y., Gong, D., Feng, Z., Liu, D., Peng, W., et al. (2017). Geochemical Characteristics of Gases from the Largest Tight Sand Gas Field (Sulige) and Shale Gas Field (Fuling) in China. *Mar. Pet. Geology.* 79, 426–438. doi:10.1016/j.marpetgeo.2016.10.021

Dai, J. X. (1992). Identification and Distinction of Various Alkane Gases. *Sci. China Ser. B-Chemistry* 35 (10), 1246–1257.

Dai, J., Zou, C., Dong, D., Ni, Y., Wu, W., Gong, D., et al. (2016). Geochemical Characteristics of marine and Terrestrial Shale Gas in China. *Mar. Pet. Geology.* 76, 444–463. doi:10.1016/j.marpetgeo.2016.04.027

Dai, J., Zou, C., Liao, S., Dong, D., Ni, Y., Huang, J., et al. (2014). Geochemistry of the Extremely High thermal Maturity Longmaxi Shale Gas, Southern Sichuan Basin. *Org. Geochem.* 74, 3–12. doi:10.1016/j.orggeochem.2014.01.018

Dong, D., Wang, Y., Huang, X., Zhang, C., Guan, Q., Huang, J., et al. (2016). Discussion about Geological Characteristics, Resource Evaluation Methods and its Key Parameters of Shale Gas in China. *Nat. Gas Geosci.* 27 (9), 1583–1601. (In Chinese with English abstract). doi:10.11764/j.issn.1672-1926.2016.09.1583

Feng, Z., Dong, D., Tian, J., Qiu, Z., Wu, W., and Zhang, C. (2018). Geochemical Characteristics of Longmaxi Formation Shale Gas in the Weiyuan Area, Sichuan Basin, China. *J. Pet. Sci. Eng.* 167, 538–548. doi:10.1016/j.petrol.2018.04.030

Feng, Z., Dong, D., Tian, J., Wu, W., Cai, Y., Shi, Z., et al. (2019). Geochemical Characteristics of Lower Silurian Shale Gas in the Changning-Zhaotong Exploration Blocks, Southern Periphery of the Sichuan Basin. *J. Pet. Sci. Eng.* 174, 281–290. doi:10.1016/j.petrol.2018.11.022

Feng, Z., Hao, F., Dong, D., Zhou, S., Wu, W., Xie, C., Cai, Y., and Li, Z. (2020). Geochemical Anomalies in the Lower Silurian Shale Gas from the Sichuan Basin, China: Insights from a Rayleigh-type Fractionation Model. *Org. Geochem.* 142, 103981. doi:10.1016/j.orggeochem.2020.103981

Freeman, C. M., Moridis, G. J., and Blasingame, T. A. (2011). A Numerical Study of Microscale Flow Behavior in Tight Gas and Shale Gas Reservoir Systems. *Transp Porous Med.* 90 (1), 253–268. doi:10.1007/s11242-011-9761-6

Guo, H., Jia, W., Peng, P. a., Zeng, J., and He, R. (2017). Evolution of Organic Matter and Nanometer-Scale Pores in an Artificially Matured Shale Undergoing Two Distinct Types of Pyrolysis: a Study of the Yanchang Shale with Type II Kerogen. *Org. Geochem.* 105, 56–66. doi:10.1016/j.orggeochem.2017.01.004

Hao, F., and Zou, H. (2013). Cause of Shale Gas Geochemical Anomalies and Mechanisms for Gas Enrichment and Depletion in High-Maturity Shales. *Mar. Pet. Geol.* 44, 1–12.

He, D. (2017). *Thermal Maturity, Composition and Origin of the Hydrocarbon Gases of the Eagle Ford Shale in Texas, USA Senior Thesis*. Columbus, OH: Ohio State University, 25.

Hu, H., Hao, F., Lin, J., Lu, Y., Ma, Y., and Li, Q. (2017). Organic Matter-Hosted Pore System in the Wufeng-Longmaxi (O 3 W-S 1 1) Shale, Jiaoshiba Area, Eastern Sichuan Basin, China. *Int. J. Coal Geology.* 173, 40–50. doi:10.1016/j.coal.2017.02.004

Huang, H., Li, R., Chen, W., Chen, L., Jiang, Z., Xiong, F., et al. (2021). Revisiting Movable Fluid Space in Tight fine-grained Reservoirs: A Case Study from Shahejie Shale in the Bohai Bay Basin, NE China. *J. Pet. Sci. Eng.* 207, 109170. doi:10.1016/j.petrol.2021.109170

Huang, H., Li, R., Jiang, Z., Li, J., and Chen, L. (2020b). Investigation of Variation in Shale Gas Adsorption Capacity with Burial Depth: Insights from the Adsorption Potential Theory. *J. Nat. Gas Sci. Eng.* 73, 103043. doi:10.1016/j.jngse.2019.103043

Huang, H., Li, R., Xiong, F., Hu, H., Sun, W., Jiang, Z., et al. (2020a). A Method to Probe the Pore-Throat Structure of Tight Reservoirs Based on Low-Field NMR: Insights from a Cylindrical Pore Model. *Mar. Pet. Geology.* 117, 104344. doi:10.1016/j.marpetgeo.2020.104344

Jenden, P. D., Hilton, D. R., Kaplan, I. R., Craig, H., and Howell, D. G. (1993). Abiogenic Hydrocarbons and Mantle Helium in Oil and Gas fields. *US Geol. Surv. Prof. paper* 1570 (1), 31–56.

Jiang, Z., Song, Y., Tang, X., Li, Z., Wang, X., Wang, G., Xue, Z., Li, X., Zhang, K., Chang, J., and Qiu, H. (2020). Controlling Factors of marine Shale Gas Differential Enrichment in Southern China. *Pet. Exploration Development* 47 (3), 661–673. doi:10.1016/s1876-3804(20)60083-0

Ko, L. T., Ruppel, S. C., Loucks, R. G., Hackley, P. C., Zhang, T., and Shao, D. (2018). Pore-types and Pore-Network Evolution in Upper Devonian-Lower Mississippian Woodford and Mississippian Barnett Mudstones: Insights from Laboratory thermal Maturation and Organic Petrology. *Int. J. Coal Geology.* 190, 3–28. doi:10.1016/j.coal.2017.10.001

Kuila, U., Mccarty, D. K., Derkowski, A., Fischer, T. B., Topór, T., and Prasad, M. (2014). Nano-scale Texture and Porosity of Organic Matter and clay Minerals in Organic-Rich Mudrocks. *Fuel* 135, 359–373. doi:10.1016/j.fuel.2014.06.036

Li, J.-L., Zhang, T.-S., Li, Y.-J., Liang, X., Wang, X., Zhang, J.-H., Zhang, Z., Shu, H.-L., and Rao, D.-Q. (2020). Geochemical Characteristics and Genetic Mechanism of the High-N2 Shale Gas Reservoir in the Longmaxi Formation, Dianqianbei Area, China. *Pet. Sci.* 17 (4), 939–953. doi:10.1007/s12182-020-00456-8

Li, J., Ma, W., Wang, Y., Wang, D., Xie, Z., Li, Z., et al. (2018). Modeling of the Whole Hydrocarbon-Generating Process of Sapropelic Source Rock. *Pet. Exploration Development* 45 (3), 461–471. doi:10.1016/s1876-3804(18)30051-x

Liu, S., Deng, B., Zhong, Y., Ran, B., Yong, Z., Sun, W., et al. (2016). Unique Geological Features of Burial and Superimposition of the Lower Paleozoic Shale Gas across the Sichuan Basin and its Periphery. *Earth Sci. Front.* 23 (1), 011–028. (in Chinese with English abstract).

Liu, Y., Tang, X., Zhang, J., Mo, X., Huang, H., and Liu, Z. (2018). Geochemical Characteristics of the Extremely High thermal Maturity Transitional Shale Gas in the Southern North China Basin (SNCB) and its Differences with marine Shale Gas. *Int. J. Coal Geology.* 194, 33–44. doi:10.1016/j.coal.2018.05.005

Loucks, R. G., Reed, R. M., Ruppel, S. C., and Hammes, U. (2012). Spectrum of Pore Types and Networks in Mudrocks and a Descriptive Classification for Matrix-Related Mudrock Pores. *Bulletin* 96, 1071–1098. doi:10.1306/08171111061

Ma, Y., Zhong, N., Yao, L., Huang, H., Larter, S., and Jiao, W. (2020). Shale Gas Desorption Behavior and Carbon Isotopic Variations of Gases from Canister Desorption of Two Sets of Gas Shales in south China. *Mar. Pet. Geology.* 113, 104127. doi:10.1016/j.marpetgeo.2019.104127

Milkov, A. V., and Etiope, G. (2018). Revised Genetic Diagrams for Natural Gases Based on a Global Dataset of >20,000 Samples. *Org. Geochem.* 125, 109–120. doi:10.1016/j.orggeochem.2018.09.002

Milkov, A. V., Faiz, M., and Etiope, G. (2020). Geochemistry of Shale Gases from Around the World: Composition, Origins, Isotope Reversals and Rollovers, and Implications for the Exploration of Shale Plays. *Org. Geochem.* 143, 103997. doi:10.1016/j.orggeochem.2020.103997

Ou, C., Li, C., Rui, Z., and Ma, Q. (2018). Lithofacies Distribution and Gas-Controlling Characteristics of the Wufeng-Longmaxi Black Shales in the southeastern Region of the Sichuan Basin, China. *J. Pet. Sci. Eng.* 165, 269–283. doi:10.1016/j.petrol.2018.02.024

Passey, Q. R., Bohacs, K. M., Esch, W. L., Klimentidis, R., Sinha, S., et al. (2010). *From Oil-Prone Source Rock to Gas-Producing Shale Reservoir-Geologic and Petrophysical Characterization of Unconventional Shale Gas reservoirs[C]// International Oil and Gas Conference and Exhibition in China*. Beijing, China: SPE.

Price, L. C. (2001). *A Possible deep-basin-high-rank Gas Machine via Water-Organicmatter Redox Reactions*. Hunter Mill: US Geological Survey. Digital Data Series, 67. (Chapter H).

Qiu, N., Feng, Q., Borjigin, T., Shen, B., Ma, Z., Yu, L., et al. (2020). Yanshanian-Himalayan Differential Tectono-thermal Evolution and Shale Gas Preservation in Dingshan Area,southeastern Sichuan Basin[J]. *Acta Petrolei Sinica* 41 (12), 1610–1622. (In Chinese with English abstract). doi:10.7623/syxb202012013

Qu, Z. (2015). *Masters Dissertation*. Guangzhou: Guangzhou Institute of Geochemistry, University of Chinese Academy of Science. (In Chinese with English abstract).Shale Gas Generation and Variation in Stable Carbon and Hydrogen Isotope Compositions.

Singh, P., Slatt, R., Borges, G., Perez, R., Portas, R., Marfurt, K., et al. (2009). Reservoir Characterization of Unconventional Gas Shale Reservoirs: Example from the Barnett Shale, Texas, U.S.A. *Okla. City Geol. Soc.* 1 (60), 15–31.

Tang, Y., and Xia, D. (2011). Quantitative Assessment of Shale-Gas Potential Based on its Special Generation and Accumulation Processes: Search and Discovery Article #40819. Available at: http://www.searchanddiscovery.com/pdfz/documents/2011/40819tang/ndx_tang.pdf.html (Accessed September 5, 2019)

Tang, Q., Zhang, M., Cao, C., Song, Z., Li, Z., and Hu, X. (2015). The Molecular and Carbon Isotopic Constrains on Origin and Storage of Longmaxi Formation Shale Gas in Changning Area, Sichuan Basin, China. *Interpretation* 3 (2), SJ35–SJ47. doi:10.1190/int-2014-0158.1

Telling, J., Lacrampe-Couloume, G., and Lollar, B. S. (2013). Carbon and Hydrogen Isotopic Composition of Methane and C2+ Alkanes in Electrical Spark Discharge: Implications for Identifying Sources of Hydrocarbons in Terrestrial and Extraterrestrial Settings. *Astrobiology* 13, 483–490. doi:10.1089/ast.2012.0915

Tilley, B., McLellan, S., Hiebert, S., Quartero, B., Veilleux, B., and Muehlenbachs, K. (2011). Gas Isotope Reversals in Fractured Gas Reservoirs of the Western Canadian Foothills: Mature Shale Gases in Disguise. *Bulletin* 95, 1399–1422. doi:10.1306/01031110103

Tilley, B., and Muehlenbachs, K. (2013). Isotope Reversals and Universal Stages and Trends of Gas Maturation in Sealed, Self-Contained Petroleum Systems. *Chem. Geology.* 339, 194–204. doi:10.1016/j.chemgeo.2012.08.002

Topór, T., Derkowski, A., Ziemiański, P., Szczurowski, J., and Mccarty, D. K. (2017). The Effect of Organic Matter Maturation and Porosity Evolution on Methane Storage Potential in the Baltic Basin (Poland) Shale-Gas Reservoir. *Int. J. Coal Geol.* 180, 46–56. doi:10.1016/j.coal.2017.07.005

Wang, F., Guan, J., Feng, W., and Bao, L. (2013). Evolution of Overmature marine Shale Porosity and Implication to the Free Gas Volume. *Pet. Exploration Development* 40, 819–824. doi:10.1016/s1876-3804(13)60111-1

Wang, X., Li, X., Wang, X., Shi, B., Luo, X., Zhang, L., Lei, Y., Jiang, C., and Meng, Q. (2015). Carbon Isotopic Fractionation by Desorption of Shale Gases. *Mar. Pet. Geology.* 60, 79–86. doi:10.1016/j.marpetgeo.2014.11.003

Wang, Y., Liu, L., Zheng, S., Luo, Z., Sheng, Y., and Wang, X. (2019). Full-scale Pore Structure and its Controlling Factors of the Wufeng-Longmaxi Shale, Southern Sichuan Basin, China: Implications for Pore Evolution of Highly Overmature marine Shale. *J. Nat. Gas Sci. Eng.* 67, 134–146. doi:10.1016/j.jngse.2019.04.020

Waples, D. W. (2000). The Kinetics of In-Reservoir Oil Destruction and Gas Formation: Constraints from Experimental and Empirical Data, and from Thermodynamics. *Org. Geochem.* 31 (6), 553–575. doi:10.1016/s0146-6380(00)00023-1

Whiticar, M. J. (1999). Carbon and Hydrogen Isotope Systematics of Bacterial Formation and Oxidation of Methane. *Chem. Geol.* 161 (1-3), 291–314. doi:10.1016/s0009-2541(99)00092-3

Wu, W., Fang, C. C., Dong, D. Z., and Liu, D. (2015). Shale Gas Geochemical Anomalies and Gas Source Identification. *Acta Petrolei Sinica* 36 (11), 1332–1340. (In chinese with English abstract). doi:10.7623/syxb201511002

Wu, W., Xie, J., Shi, X., Zhao, S., Ji, C., Hu, Y., et al. (2017). Accumulation Condition and Exploration Potential for Wufeng-Longmaxi Shale Gas in Wuxi Area, Northeastern Sichuan Basin. *Nat. Gas Geosci.* 28 (5), 734–743. (In chinese with English abstract). doi:10.11764/j.issn.1672-1926.2017.04.009

Xi, Z., Tang, S., Zhang, S., Lash, G. G., and Ye, Y. (2022). Controls of marine Shale Gas Accumulation in the Eastern Periphery of the Sichuan Basin, South China. *Int. J. Coal Geology.* 251, 103939. doi:10.1016/j.coal.2022.103939

Xia, X., Chen, J., Braun, R., and Tang, Y. (2013). Isotopic Reversals with Respect to Maturity Trends Due to Mixing of Primary and Secondary Products in Source Rocks. *Chem. Geology.* 339, 205–212. doi:10.1016/j.chemgeo.2012.07.025

Xia, X., and Gao, Y. (2018). Depletion of 13C in Residual Ethane and Propane during thermal Decomposition in Sedimentary Basins. *Org. Geochem.* 125, 121–128. doi:10.1016/j.orggeochem.2018.09.003

Xin, C., Chen, L., Guo, X., and Wang, C. (2019). Geochemical Characteristics of Shale Gas in the Silurian Longmaxi Formation, Jiaoshiba Area, Southeast Sichuan Basin, China. *Energy Fuels* 33 (9), 8045–8054. doi:10.1021/acs.energyfuels.9b01305

Xu, C., Jia-yu, R., Yue, L., and Boucot, A. J. (2004). Facies Patterns and Geography of the Yangtze Region, South China, through the Ordovician and Silurian Transition. *Palaeogeogr. Palaeoclimatol. Palaeoecol.* 204 (3-4), 353–372. doi:10.1016/s0031-0182(03)00736-3

Xu, E., Li, Z., and Yang, Z. (2015). Thermal and Hydrocarbon Generation History of Wufeng and Longmaxi Shales in Pengshui Area, Eastern Sichuan Basin: A Well PY1 Case Study. *Pet. Geology. Exp.* 37 (4), 494–499. (In Chinese with English abstract).

Xu, L., Wang, Y., Liu, L., Chen, L., and Chen, J. (2019). Evolution Characteristics and Model of Nanopore Structure and Adsorption Capacity in Organic-Rich Shale during Artificial thermal Maturation: A Pyrolysis Study of the Mesoproterozoic Xiamaling marine Shale with Type II Kerogen from Zhangjiakou, Hebei, China. *Energy Exploration & Exploitation* 37 (1), 493–518. doi:10.1177/0144598718810256

Yang, R., He, S., Hu, Q., Hu, D., and Yi, J. (2017). Geochemical Characteristics and Origin of Natural Gas from Wufeng-Longmaxi Shales of the Fuling Gas Field, Sichuan Basin (China). *Int. J. Coal Geology.* 171, 1–11. doi:10.1016/j.coal.2016.12.003

Zhang, M., Tang, Q., Cao, C., Lv, Z., Zhang, T., Zhang, D., et al. (2018). Molecular and Carbon Isotopic Variation in 3.5 Years Shale Gas Production from Longmaxi Formation in Sichuan Basin, China. *Mar. Pet. Geology.* 89, 27–37. doi:10.1016/j.marpetgeo.2017.01.023

Zhao, W., Jia, A., Wei, Y., Wang, J., and Zhu, H. (2020). Progress in Shale Gas Exploration in China and Prospects for Future Development. *China Pet. Exploration* 25 (1), 31. doi:10.3969/j.issn.1672-7703.2020.01.004

Zhao, W., Wang, Z., Wang, H., Li, Y., Hu, G., and Zhao, C. (2011). Further Discussion on the Connotation and Significance of the Natural Gas Relaying Generation Model from Organic Matter. *Pet. Exploration Development* 38 (2), 129–135. doi:10.1016/s1876-3804(11)60021-9

Zhao, W., Zhang, S., He, K., Zeng, H., Hu, G., Zhang, B., et al. (2019). Origin of Conventional and Shale Gas in Sinian-Lower Paleozoic Strata in the Sichuan Basin: Relayed Gas Generation from Liquid Hydrocarbon Cracking. *Bulletin* 103 (6), 1265–1296. doi:10.1306/11151817334

Zou, C., Dong, D., Wang, S., Li, J., Li, X., Wang, Y., et al. (2010). Geological Characteristics and Resource Potential of Shale Gas in China. *Pet. exploration Dev.* 37 (6), 641–653. doi:10.1016/s1876-3804(11)60001-3

Zou, C., Dong, D., Wang, Y., Li, X., Huang, J., Wang, S., et al. (2016). Shale Gas in China: Characteristics, Challenges and Prospects (II). *Pet. Exploration Development* 43 (2), 182–196. doi:10.1016/s1876-3804(16)30022-2

Zou, C., Zhao, Q., Cong, L., Wang, H., Shi, Z. S., Wu, J., et al. (2021). Development Progress, Potential and prospect of Shale Gas in China. *Nat. Gas Industry* 41 (1), 1–14. doi:10.3787/j.issn.1000-0976.2021.01.001

Zumberge, J., Ferworn, K., and Brown, S. (2012). Isotopic Reversal ('rollover') in Shale Gases Produced from the Mississippian Barnett and Fayetteville Formations. *Mar. Pet. Geology.* 31, 43–52. doi:10.1016/j.marpetgeo.2011.06.009

Conflict of Interest: Author PW was employed by the Sinopec Green Source Thermal Energy Development Co., Ltd.

The remaining authors declare that the research was conducted in the absence of any commercial or financial relationships that could be construed as a potential conflict of interest.

Publisher's Note: All claims expressed in this article are solely those of the authors and do not necessarily represent those of their affiliated organizations, or those of the publisher, the editors and the reviewers. Any product that may be evaluated in this article, or claim that may be made by its manufacturer, is not guaranteed or endorsed by the publisher.